Journal of Catalysis 265 (2009) 109–116

Contents lists available at ScienceDirect

Journal of Catalysis

journal homepage: www.elsevier.com/locate/jcat

Biomass into chemicals: One pot-base free oxidative esterification of 5-hydroxymethyl-2-furfural into 2,5-dimethylfuroate with gold on nanoparticulated ceria

O. Casanova, S. Iborra, A. Corma *

Instituto de Tecnología Química (UPV-CSIC), Avda dels Tarongers s/n, Universitat Politècnica de València, 46022 Valencia, Spain

ARTICLE INFO

Article history:
Received 28 January 2009
Revised 30 March 2009
Accepted 21 April 2009
Available online 28 May 2009

Keywords:
Catalysis
5-Hydroxymethyl-2-furfural
2,5-Dimethylfuroate
Gold
Ceria

ABSTRACT

2,5-Dimethylfuroate (DMF) is a valuable biomass derivative that can replace oil dependent PET polymers. 5-Hydroxymethyl-2-furfural (HMF) has been selectively converted into DMF (99 mol% yield) under mild conditions (65–130 °C, 10 bar O_2) in the absence of any base, by using gold nanoparticles on nanoparticulated ceria. The catalyst can be reused several times without any loss of activity or selectivity. The absence of metal leaching has been checked by the three-phase test. A full reaction scheme has been established and it has been found that the rate-limiting step of the reaction is the alcohol oxidation into aldehyde. After this, the reaction proceeds via aldehyde conversion into hemiacetal and further oxidation into the corresponding ester. Additionally, the effect of temperature, substrate-to-catalyst ratio, alcohol and water has been studied in an attempt to explain the catalytic behaviour of the Au–CeO_2.

1. Introduction

The production of fine chemicals, polymer precursors and petrol-derived commodities from biomass can contribute to diminish our current dependence on non-renewable energy sources, and chemical routes for catalytic biomass transformations have been recently reviewed [1–3]. It has been presented that one of the foremost natural sources of potentially relevant chemicals are sugars, and good results have been achieved in converting fructose into liquid alkanes and the production of a key intermediate such as 5-hydroxymethyl-2-furfural (HMF) by homogeneous Brönsted acid dehydration [4]. This compound is regarded as a key element for the development of several derivatives with multiple applications, e.g. pharmaceuticals, antifungals and polymer precursors [1]. Among these applications, the synthesis of polymer precursors can be of interest. One of the monomers, whose volume of production is constantly increasing is terephthalic acid (commonly used in the manufacture of PET [5]), which according to Gandini and co-workers [6] can be replaced by 2,5-furandicarboxylic acid (FDCA). The latter replacement has been recently emphasized due to improvements observed in terms of heat resistance and mechanical properties [7]. Several attempts to synthesize FDCA have been reported in the literature [8–11], but it is difficult to handle due to its low solubility in most industrial solvents [5]. However, such difficulty can be overcome by substituting FDCA by its corresponding ester, i.e. dimethylfuroate (DMF), which is readily soluble in most common solvents. Therefore, a process that is able to convert HMF into DMF can have an impact on the polymer industry.

The idea of synthesizing inexpensive DMF should embody a process wherein the oxidation of alcohol into aldehyde, the hemiacetal formation and further hemiacetal oxidation should occur in a one-pot system to avoid the costly isolation and purification of the intermediates. It is well known that alcohol oxidation is usually a limiting step, whenever successive aldehyde oxidation is desired [12]. Currently, the former oxidation step can be accomplished by Pd [13], Au and Au–Pd supported catalysts [14–16], particularly using gold nanoparticles supported onto nanoparticulated ceria (Au–CeO_2). This type of catalyst is of general use, able to work at low temperature, short reaction time, low amounts of catalyst, with environmentally friendly solvents and with O_2 as oxidant [17–21]. The key aspect of the catalytic performance of Au–CeO_2 lies on the variation of the chemical properties when particle size decreases. External atoms have the ability to bind with adsorbates due to the presence of unsaturations in their valence. Clearly, when the particle size is reduced, then the external-to-internal atom ratio increases. Therefore, particles in the nanoscale (nanoparticles thereafter) present a high population of unsaturations, responsible for specific chemical properties. In the case of CeO_2, these unsaturations can be understood as defect sites, mainly oxygen vacancies, which make the stoichiometric formula CeO_2 like CeO_{2-x} being x

* Corresponding author. Fax: +34 963877809.
E-mail address: acorma@itq.upv.es (A. Corma).

0021-9517/$ - see front matter © 2009 Elsevier Inc. All rights reserved.
doi:10.1016/j.jcat.2009.04.019

related to oxygen vacancies and the presence of Ce^{III}. Similarly, if metal nanoparticles (such as Au) are supported onto nanoparticulated ceria, then the immediate consequence is again an increase in the population of defects, which will enhance a given property (adsorption capacity, redox potential, etc.) [22].

An important role played by nanoparticulated ceria in alcohol oxidation was noticed when different catalysts having the same composition and gold particle size, but different supports (TiO_2, Fe_2O_3, C, etc.) showed different catalytic performances. This was related to the fact that nanoparticulated ceria was able to adsorb oxygen, due to its oxygen vacancies, hence boosting reoxidation steps within the mechanism. On the other hand, the Lewis acid character of non-fully saturated cerium atoms becomes beneficial for alcohol oxidation, and furthermore its interaction with gold nanoparticles stabilizes positive gold atoms, responsible for the initiation steps of the reaction [17].

Recently, Christensen and co-workers [23] have reported very interesting results on HMF oxidation–esterification into DMF (99 mol% yield) using Au–TiO_2 catalyst at 130 °C in MeOH with the aid of MeONa. Therein, a clear emphasis was laid on the role played by MeONa, so that in its absence the reaction may not be completed after longer reaction times, while the addition of a base to HMF oxidation would make the process less green and more expensive. Moreover, it has been reported that storage conditions (light and temperature) may negatively alter the Au–TiO_2 properties and this has been illustrated in oxidative reactions [24]. All these factors led us to consider the possibility of searching for a material with better stability and catalytic activity.

In the present work we will show that base-free environmentally friendly one-pot synthesis of DMF (and other esters thereof) has been achieved with Au–CeO_2 and the catalytic activity will be compared with that of Au–TiO_2, which is regarded as the most efficient one in the literature [23]. The molecular intermediates of the reaction have been determined, and a global network has been established. Kinetic parameters of the process were studied together with the reusability and stability of Au–CeO_2 by means of successive reuses, chemical analysis and the three-phase reaction test.

2. Experimentals and methods

2.1. Synthesis of catalysts

Synthesis of 2.1 wt% Au–CeO_2 catalyst: The preparation of nanoparticulated ceria was carried out following the reported procedure [25]. In short, an aqueous solution of $Ce(NO_3)_4$ (375 mL, 0.8 M) was treated, under stirring and at ambient temperature, with an aqueous solution of ammonia (1.12 L, 0.8 M). The colloidal dispersion of CeO_2 nanoparticles was heated in a PET vessel at 100 °C for 24 h. The resulting yellow precipitate was filtered and dried under vacuum overnight. The cerium oxide synthesized has, owing to the small size of the nanoparticles, a very high surface area (180 m^2/g).

Gold was deposited on the nanoparticulated ceria by using the following procedure (same as when no-nanometric ceria was used): a solution of $HAuCl_4{\cdot}3H_2O$ (350 mg) in deionized water (160 mL) was brought to pH 10 by the addition of a solution of NaOH 0.2 M. Once the pH value was stable the solution was added to a gel containing colloidal CeO_2 (4.01 g) in H_2O (50 mL). After adjusting the pH of the slurry at a value of 10 by the addition of a 0.2 M solution of NaOH 0.2 M, the slurry was continuously stirred vigorously for 18 h at RT. The Au–CeO_2 solid was then filtered and exhaustively washed with several litres of distilled water until no traces of chlorides were detected by the $AgNO_3$ test. The catalyst was dried under vacuum at room temperature for 1 h. The total Au content of the final catalyst was 2.1 wt% as determined by chemical analysis and the average metal size of the nanoparticles was 3.5 nm from TEM. This Au–CeO_2 catalyst is commercially available at http://www.upv.es/itq.

Synthesis of 1.5 wt% Au–C catalyst: A colloidal solution of gold nanoparticles stabilized by polyvinylalcohol was deposited on activated carbon (KB-B-100, provided by Aldrich), following the procedure reported by Porta et al. [26], under vigorous stirring an aqueous solution of $HAuCl_4$ (2 L, 100 μg mL^{-1}). To this, a fresh solution of $NaBH_4$ (38 mL, 0.1 M) was added. The Au nanoparticles generated were immobilized simply by adding the active carbon (2 g) into the metal dispersion. After 1 h the slurry was filtered and the total gold adsorption was checked by atomic absorption spectroscopy of the filtrate. The average metal size of the nanoparticles was 3.5 nm.

1 wt% Au–TiO_2 and 4.5 wt% Au–Fe_2O_3 catalysts: They were directly purchased from TEK and WGC, respectively, and were used as received. In both cases, the average metal size of the nanoparticles was 3.5 nm.

2.2. Synthesis of compounds 5-hydroxymethyl furoic acid methyl ester and 5-hydroxymethyl furfural dimethyl acetal

5-Hydroxymethyl furoic acid methyl ester was prepared as follows: 400 mg HMF was dissolved in 40 mL MeOH, 50 mg MeONa (35 wt% solution in MeOH) and 140 mg Au–TiO_2 were added under vigorous stirring and refluxed at (65 °C). Then, air was bubbled into the reaction mixture at 0.5 mL/s for ca. 12 h. The reaction was complete after this time as checked by GC/MS. After reaction the catalyst was filtered off and MeOH contained in the filtrate was evaporated and the remaining reddish concentrate (>95% yield) was used as prepared.

5-Hydroxymethyl furfural dimethyl acetal was prepared as follows: 500 mg HMF was dissolved in 25 mL MeOH and 100 mg calcined and dehydrated Al–beta zeolite (Si/Al = 12.5 mol/mol, CP806) were added under vigorous stirring and refluxed at (65 °C) for 15 min. After reaction the catalyst was filtered off and MeOH contained in the filtrate was evaporated and the remaining yellowish concentrate (>96% yield according to GC/MS analysis) was used as prepared without any further purification.

2.3. Three-phase test

The reactant for the three-phase test was prepared using the following procedure: first, the imine reactant was obtained by contacting 4 g aminofunctionalized silica (Aldrich, 1 mmol NH_2/g solid) with 1 g HMF dissolved in 50 mL CH_2Cl_2, at its reflux temperature for 4 h; second, the imine was reduced with $NaBH_4$ (1.5 equiv.) in ethanol at 5 °C for 2 h. The solids were collected by vacuum filtration at room temperature, exhaustively washed with the same solvent and dried overnight at 60 °C. The product for the three-phase test was prepared in a similar manner to the reactant, but using diformylfurane instead of HMF and the reduction step was not carried out.

The three-phase test was carried out by mixing 1 g of the three-phase test reactant, as explained before, under the conditions indicated in the catalytic experiments. For the homogeneous test with the three-phase test reactant, $AuCl_3$ was used as a catalyst, under the same conditions as indicated in the catalytic experiments.

2.4. Catalytic experiments

0.2 g HMF, 16 g (20 mL) methanol and the appropriate amount of freshly synthesized catalyst (HMF/Au mol ratio of 300, unless otherwise stated) were loaded into a teflon-lined autoclave (volume 30 mL). Afterwards, the reactor was sealed, pressurized at 10 bar with N_2 and heated up to the required temperature. Then, oxygen was bubbled into the reaction mixture at a constant flow-

rate of 0.33 mL/s keeping constant pressure by means of a back-pressure-regulator. The mixture was stirred at ca. 1000 rpm. The progress of the reaction was followed by taking samples at regular periods and was analyzed by GC. Nitrobenzene was used as the external standard.

2.5. Analytical systems

IR spectra were performed using a Nicolet 750 spectrophotometer. The spectra were obtained in the region between 3800 and 400 cm^{-1} with a resolution of 4 cm^{-1} by accumulating 40 scans, prior in situ dehydration of the sample at 100 °C.

The content of organic (wt% C, H, N, S) was measured by elemental analysis using EA-1108 CHNS Fisons analyzer and sulphanilamide as standard. Metal loading in the case of Au–C was determined by atomic absorption spectrophotometry, previous sample disgregation with a mixture of HF/HNO_3. After dilution of the resulting solution with Milli Q water, analyses were performed with a Varian-10 plus Atomic Absorption Spectrometer (+/−0.01 ppm error). Chemical analysis of Au–CeO_2 was carried out using a Philips MiniPal 25 fm Analytic X-ray apparatus and the corresponding calibration plot.

Gas chromatography (GC) analyses were performed with a Varian 3300 chromatograph equipped with a flame ionization detector and the capillary column was TRB-5 (5% crosslinked phenylmethyl silicone) (sizes 30–0.25–0.25) (Teknokroma). Mass spectra were performed by GC–MS (HP Agilent 5973 with a 6980 mass selective detector).

3. Results and discussion

3.1. Reaction network for HMF oxidation–esterification to DMF

HMF oxidation–esterification was performed in methanol, at 130 °C and 10 bar O_2 using Au–CeO_2 as a catalyst. Following the evolution of the reaction with time, different compounds were detected which are presented in Scheme 1, whereas Fig. 1 displays the kinetic curves. Firstly, it can be seen that the monoester alcohol **3** concentration increases up to a maximum of ca. 60 mol% yield, decreasing after the first hour of reaction. This behaviour allows us to consider the monoester alcohol **3** as a disguised primary and unstable product. Secondly, the acetal alcohol **4** appears as a disguised primary and unstable compound [27]. The monoester acetal **9** appears in the kinetics profile, when **3** and **4** concentrations are decreasing, showing their disguised secondary character. However, **9** is a minoritary product, because its maximal yield is

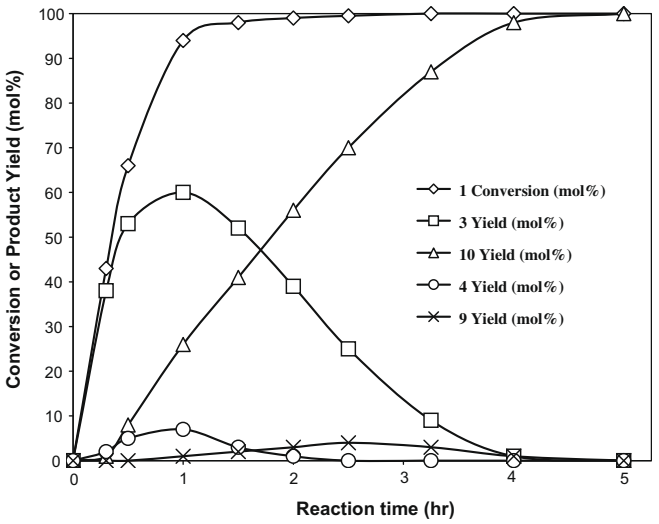

Fig. 1. Kinetics plot for the oxidation–esterification of **1** into **10** at 130 °C, 10 bar bubbled O_2 at 0.33 mL/s using Au–CeO_2 (**1**/Au mol ratio 300) as a catalyst.

reached at ca. 4 mol% after 2.5 h, and then it decreases, showing its unstable behaviour. Finally, diester **10**, which is a secondary product increases gradually its concentration in the reaction medium achieving 99 mol% after 5 h. Other compounds such as aldehyde ester **5** and aldehyde acetal **6** were detected at the trace level.

Taking into account the kinetic behaviour of the different compounds presented in Fig. 1, a reaction network is presented in Scheme 2. It can be seen that **3** and **4** are derived from the same hemiacetal intermediate **2** (non-detectable through GC), i.e. they follow the oxidation and acetalization of **2**, respectively. It is remarkable that between these two reactions, **2** is more prone to oxidation rather than to acetalization, as the maximal concentration of **3** is much higher than **4**. On the other hand, monoester acetal **9**, which ends up being further oxidized into the diester **10**, can be formed from the two pathways opened separately by the disguised primary products indicated before. More specifically, after **3** is formed, it is gradually oxidized into the monoester aldehyde **5**. Then, after its hemiacetalization into **7**, most of it is converted into the final desired product **10**, while a fraction may be transformed into **9**, which is reoxidized into **10**, as shown in the right-hand pathway in Scheme 2. In order to find out if the oxidation of the reactant into **3** or, on the contrary, it is the transformation of **3** into the final product the controlling reaction step, we have re-

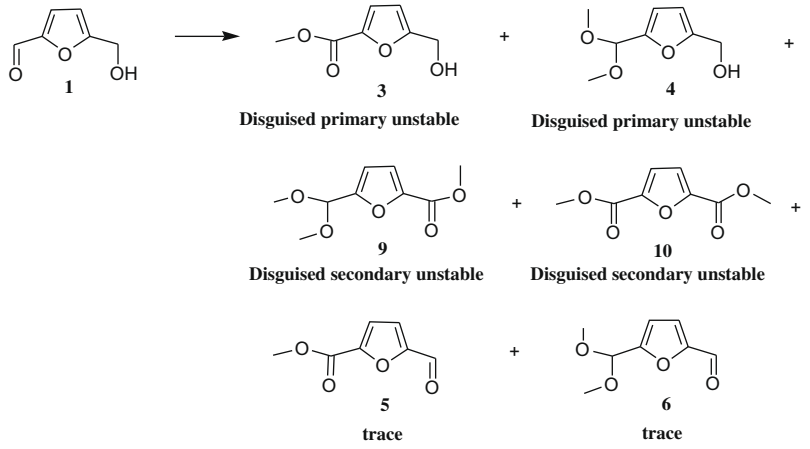

Scheme 1. Detected products in HMF oxidative esterification with MeOH.

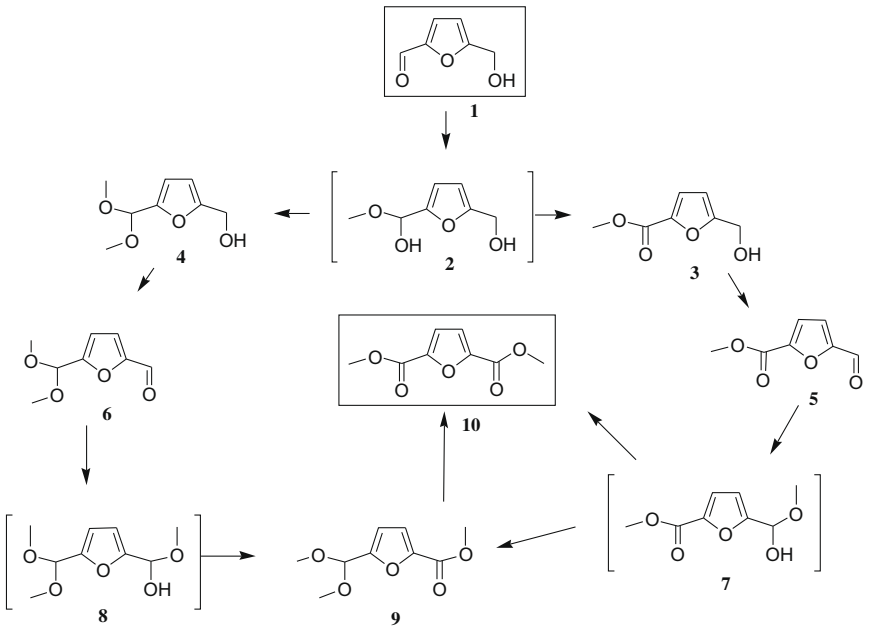

Scheme 2. Proposed **1** oxidation–esterification pathway.

acted the compound **3** under the same reaction conditions. Then, from the results given in Table 1, one can see that, when the oxidation was started from either **1** or **3**, a similar reaction time is required to reach 99 mol% yield to **10**, which means that the alcohol oxidation into aldehyde is the limiting step.

Table 1
Catalytic activity of Au–CeO_2 towards **10** formation starting from **1** and **3**.[a]

Exp.	Reactant	Product	Time (h)	Conversion (mol%)	Selectivity (mol%)
1	**1**	**10**	5	>99	>99
2	**3**	**10**	2	70	>99
			4	>99	>99

[a] Reaction conditions: 1.59 mmol **1** or **3** in 20 mL MeOH; 50 mg Au–CeO_2 (2.1 wt% Au) (**1**/Au mol ratio of 300) at 130 °C, 10 bar bubbled O_2 at 0.33 mL/s constant flowrate.

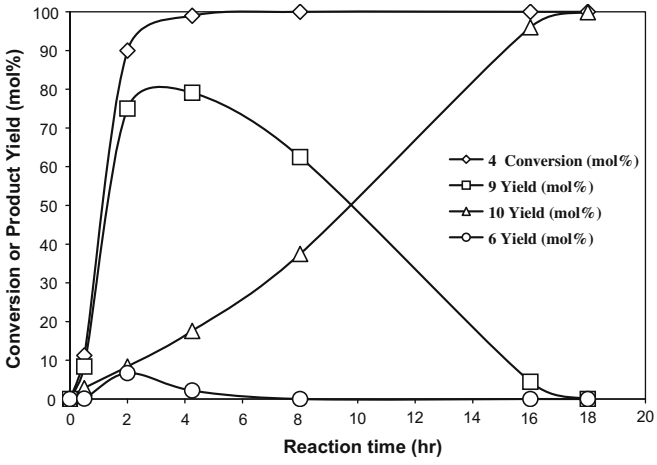

Fig. 2. Kinetics plot for the oxidation-esterification of **4** into **10** at 130 °C, 10 bar bubbled O_2 at 0.33 mL/s using Au–CeO_2 (**4**/Au mol ratio 300) as a catalyst.

If now we follow the second reaction route going through the compound **4**, then the acetal aldehyde **6** is formed, which is rapidly transformed into the hemiacetal **8**. Most of this is oxidized into **9** and finally converted into **10**. In order to rule out the possibility that compound **4** reacts to **3**, we carried out the reaction starting from pure compound **4**. The kinetics of this reaction route is shown in Fig. 2, therein the accumulation of **9** can be clearly seen, followed by the acetal oxidation. As seen in Scheme 2, compound **9** is an obligatory stage for the two reaction pathways.

The effect of the presence of different substituents in the 5-furane on the rate of oxidation of the 2-hydroxymethyl group can be seen from the results given in Table 2. When using 4-substituted-benzyl alcohol type substrates [19,28], the presence of ring deactivating groups, such as dimethoxymethyl and methylcarboxy (in **4** and **3**, respectively), decreases the rate of oxidation. In fact, after 2 h, yields to **10** are lower (74.6 and 72 mol%, respectively) than when no ring substituent was present as in **11** (Scheme 3) (91 mol% yield to **15**). Certainly, **11** follows an analogous oxidation–esterification pathway to **1**, as shown in Scheme 3.

Therefore, it can be said that Au–CeO_2 is a selective catalyst that favours the oxidation of the hemiacetal into ester and the oxidation of alcohol into aldehyde, rather than the reoxidation of the acetal into the ester. Undoubtedly, the former process is thermodynamically more favoured owing to the high stability of acetals.

3.2. Comparative study of Au–CeO_2 performance with Au nanoparticles onto different supports

Table 3 presents the initial activity of different catalysts (Au–CeO_2, Au–TiO_2, Au–Fe_2O_3 and Au–C) for the oxidation and esterification of **1**–**10** in MeOH (entries 1–4). Meanwhile in Fig. 3, we describe the kinetic behaviour of Au–CeO_2 and Au–TiO_2 without the presence of a base. As can be deduced from the results in Table 3, in the absence of base (entry 4), Au–CeO_2 is the most active catalyst of the group (>99 mol% yield to **10**, after 5 h). The values of TOF_1 and TOF_2 calculated from the conversion of **1** and yield to **10**, respectively, reveal (Table 3) that although Au–C (entry 3) is the most active catalyst (TOF_1 480 h^{-1}), both TOF_2 and the yield towards **10** after 24 h are rather low (0.5 h^{-1} and 7.6 mol%, respectively). Au–TiO_2 catalyst (entry 2) is less active than Au–C and it

Table 2
Influence of the furane substituent group on hydroxymethyl substituent group oxidation into methyl ester.[a]

Exp.	Reactant	Product	Time (h)	Conversion (mol%)	Selectivity to product (mol%)
1	**11**	**15**	2	>99	91
2	**4**	**9**	2	91	82
3	**3**	**10**	2	72	>99

[a] Reaction conditions: 1.59 mmol reactant in 20 mL MeOH; 50 mg Au–CeO_2 (2.1 wt% Au) (reactant/Au mol ratio of 300) at 130 °C, 10 bar bubbled O_2 at 0.33 mL/s constant flowrate.

displays lower TOF_2 (57 h^{-1}) than Au–CeO_2 (137 h^{-1}). Furthermore, the kinetic curves given in Fig. 3 clearly shows that Au–CeO_2 allows to obtain 100% yield to **10** in 5 h reaction time. Meanwhile with the Au–TiO_2 reported in [23], only 40% yield to **10** is achieved in 5 h, and after 24 h the yield is still 96%. Au–Fe_2O_3 catalyst (entry 1) showed very poor activity. The sole presence of nanoparticulated CeO_2 under oxidizing conditions (entry 6) resulted in the formation of large amounts of acetal **4**, together with 4 mol% yield diformylfurane (DFF). Similarly, when N_2 was bubbled with Au–CeO_2 catalyst (entry 5), the acetal **4** was the predominant product. Despite the absence of oxygen, 3.8 mol% of **3** was detected in the latter experiment. The fact that without oxygen some of the substrate could be oxidized is due to the fact that nanoparticulated cerium oxide acts as oxygen supplier [29–31], something consistent with the idea of considering this nanometric support as an oxygen pump, releasing and adsorbing oxygen through a redox process where Ce^{+4}/Ce^{+3} is involved. As seen in Table 3, when nonanometric CeO_2 (entry 7) was used to support gold nanoparticles, it took 3 days to reach 85 mol% **10**. Results on the comparative behaviour of Au–CeO_2 point at the formation of peroxo and superoxo species in monoelectronic defects of nanocrystalline ceria.

Therefore, the catalytic behaviour of gold promoted by the appropriate support containing Lewis acid sites resulted to be an optimal combination to perform the reaction in high yields.

3.3. Stability and reusability of Au–CeO_2 catalysts

Catalyst recyclability was checked by successive reuses of the catalyst under the same reaction conditions. To do that, the catalyst was recovered by vacuum filtration and successive washing with methanol and drying overnight. Calcination of adsorbed organic compounds was avoided since it could cause gold agglomeration into larger and inactive particles. The results of catalyst recycling are shown in Fig. 4. As it can be seen, after the first use, the time required to reach similar levels of yield towards **10** (>96 mol%) than the fresh catalyst was nearly twice and the initial rate of **1** conversion was almost halved. This is probably due to the presence of 11 wt% organic material after the first use that increases up to 15 wt% after the fourth use. Unfortunately, the adsorbed organic was resistant to Sohxlet extraction with methanol. Nevertheless, a full oxidation of the organic on the catalyst was performed at 250 °C in air for 12 h. The regenerated catalyst contained <5% organic and the activity was almost totally restored, as seen in Fig. 4 (cycle 5).

Catalyst stability from the point of view of gold leaching has been tested by two different procedures. Firstly, the gold content in the used catalysts was determined by X-ray fluorescence, and taking into account the contribution in weight of adsorbed organic

Table 3
Oxidation–esterification of **1** using Au nanoparticles onto different supports at 130 °C, 10 bar O_2 in methanol.

Exp.	Catalyst	TOF_1[a] (h^{-1})	TOF_2[b] (h^{-1})	T (h)	Conv. (mol%)	Yield (mol%)[c]		
						3	**10**	**4**
1	Au–Fe_2O_3	120	4	24	94	34.7	6.2	17.5
2	Au–TiO_2	305	57	3	97	49	30	2
				24	>99	3.7	96.3	0
3	Au–C	480	0.5	24	96	20.2	7.6	17.4
4	Au–CeO_2	320	137	2	98	37	54	1
				5	>99	0	>99	0
5	Au–CeO_2[d]	–	–	24	58	3.8	0	51.8
6	CeO_2	–	–	24	61	0	0	53.1
7	Au–CeO_2[e]	155	10	72	>99	0	85	15

[a] Calculated as moles of converted **1** divided by reaction time (15 min) and moles of Au.
[b] Calculated as moles of formed **10** divided by reaction time (15 min) and moles of Au.
[c] Other by-products which complete molar balance are the following: 5-methoxymethyl-2,2-dimethoxylfurane, 5-methoxymethyl-2-methylfuroate and **6**.
[d] Oxygen was replaced by nitrogen.
[e] No-nanometric CeO_2 was used as support.

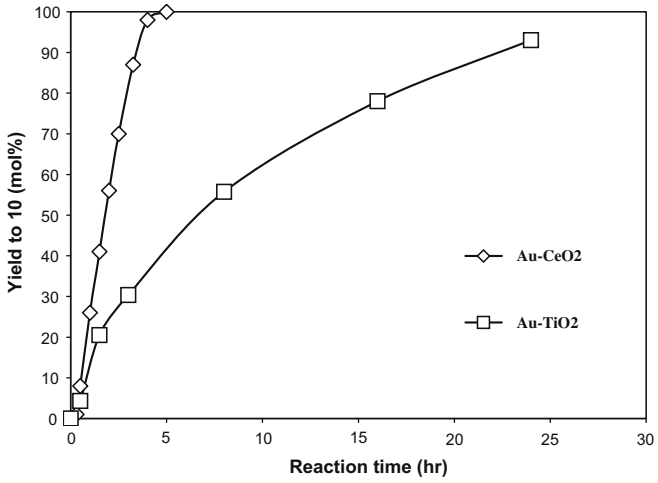

Fig. 3. Kinetics plot for the yield of **10** at 130 °C, 10 bar bubbled O_2 at 0.33 mL/s using Au–CeO_2 and Au–TiO_2 (**1**/Au mol ratio 300) as catalysts.

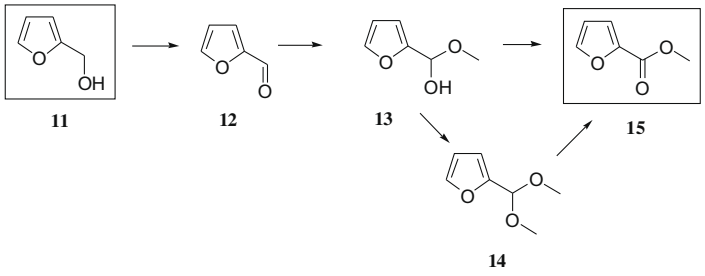

Scheme 3. Proposed **11** oxidation–esterification pathway.

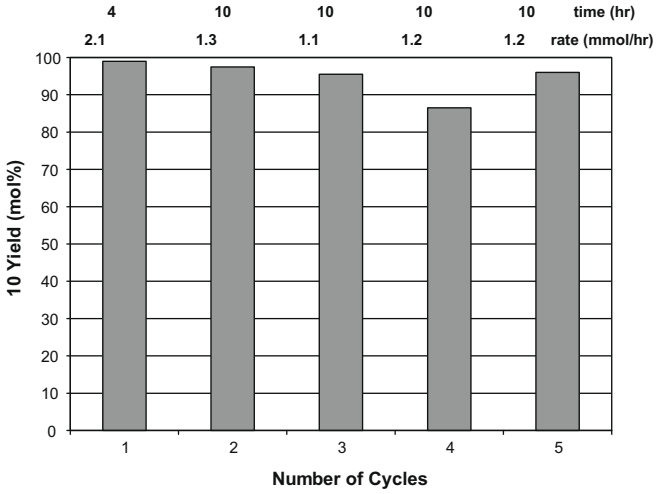

Fig. 4. Yield of **10** (mol%) with successive reuses of Au–CeO_2. The numbers above the bar chart stand for the reaction time required for achieving said yield and the initial rates of **1** conversion for each cycle.

material, leaching of gold was not detected after catalyst reuses. In agreement with this, no traces of gold were detected in the reaction filtrate. In second and definitive leaching test, the three-phase reaction test was applied [32,33]. According to the procedure explained in the experimental part, the IR results on the three-phase test are shown in Fig. 5. Compound **1** reacted with aminofunctionalized silica to yield the corresponding imine. Due to the instability of imine-supported-**1** (line c), further reduction into secondary amine (line d) was necessary in order to avoid the substrate from passing to the solution. The latter curve corresponds to the actual three-phase test reactant. After the test was accomplished, the IR spectrum of used solids (line e) is shown. If we compare the initial and final solid, no trace of bands corresponding to the ester or aldehyde (line f) can be observed. However, when the reaction was performed using homogeneous gold ($AuCl_3$), the bands corresponding to oxidation products appeared (line g). Therefore, it can be stated that under the reaction conditions, Au–CeO_2 did not suffer from metal leaching and further redeposition on the surface, known as "boomerang effect".

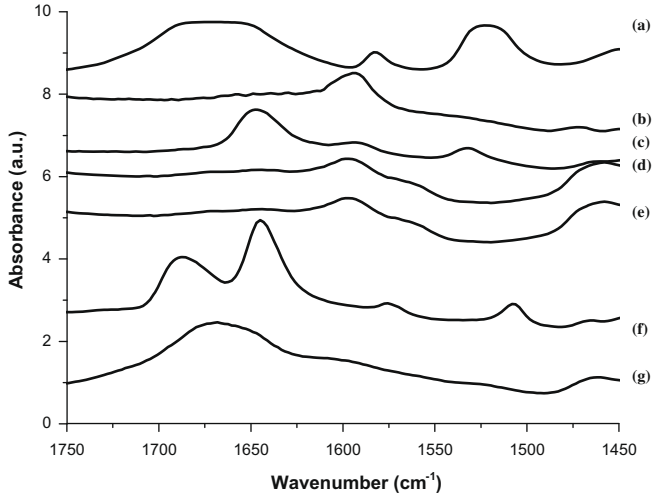

Fig. 5. IR spectra for (a) **1** reagent; (b) SiO_2–NH_2 initial support; (c) silica-supported imine reagent **1**; (d) silica-supported amine reagent before the three-phase-test; (e) silica-supported amine reagent after the three-phase test; (f) silica-supported imine product (formyl-furane); (g) silica-supported amine reagent after the homogeneous reaction.

3.4. Optimization of reaction conditions: HMF/Au ratio and temperature

The evolution of the yield of the desired diester product **10** with reaction time, working at 185, 300 and 760 reactant to gold molar ratio is shown in Fig. 6. As can be observed there, the time required to reach >99 mol% yield to **10**, was ca. 2.5, 5 and 30 h, respectively, being the initial reaction rate, directly proportional to the concentration of catalyst.

The variation of the conversion of **1** with time is plotted in Fig. 7 for three different temperatures (80, 100 and 130 °C) at a **1**/Au mol ratio of 300. Clearly, the higher the temperature, the higher initial rate and, consequently, 130 °C was regarded here as a suitable temperature to perform the reaction. An Arrhenius plot of the logarithm of the initial rate gives an apparent activation energy of

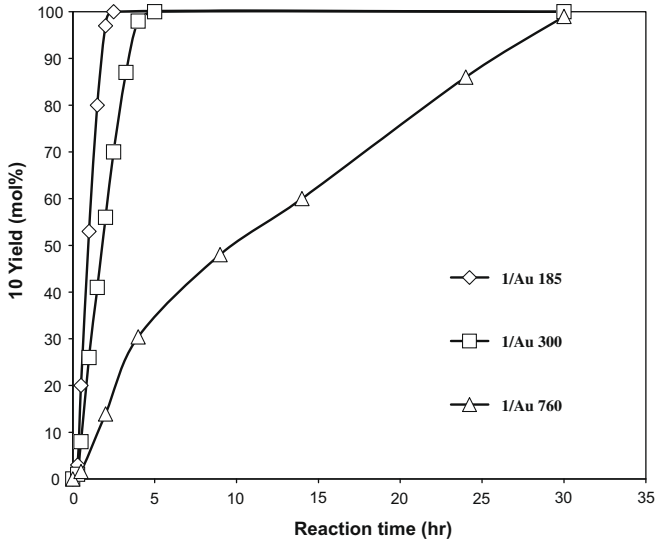

Fig. 6. Effect of **1**/Au mol ratio on **10** yield at 130 °C and 10 bar bubbled O_2 in MeOH using Au–CeO_2 catalyst.

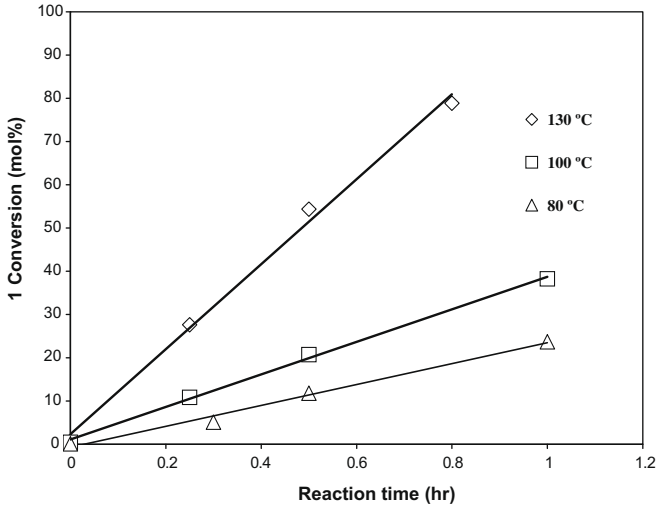

Fig. 7. Effect of temperature on **1** conversion at **1**/Au mol ratio 300 and 10 bar bubbled O_2 in MeOH using Au–CeO_2 catalyst.

34 kJ/mol which is in the same order as for the oxidation of other alcohols such as *p*-methylbenzyl alcohol using Au–CeO_2 [18].

3.5. Effect of the alcohol

Several short chain alcohols (methanol, ethanol and *n*-butanol) were tested for the oxidation–esterification of **1**, and the results are given in Fig. 8. It can be clearly seen that methanol was the most suitable alcohol (which here plays the role of reactant and solvent simultaneously) to obtain the corresponding ester. It has to be noted that, as reported in the literature [23], between 0.3 and 0.5 mol MeOH was oxidized per mol of reactant, being the typical oxidation products such as methyl formate, formaldehyde dimethyl acetal and CO_2. It was noticed that when ethanol or butanol was loaded, then initial rate decreased and time required for full conversion was enhanced considerably. Also large amounts of acetals from ethanol and *n*-butanol were formed. Au–CeO_2 catalyst, by being a good alcohol oxidizer, was capable of performing these side-reactions due to the easiness to form metal–alcoholate adducts when increasing the alkyl chain.

3.6. Effect of water

Although Au–CeO_2 has proved to withstand water to perform catalytic oxidations of alcohols [17], we have studied the effect of water concentration on the catalytic performance, and the results are given in Fig. 9. A negative effect of water can be observed when the initial rate was smaller and the concentration of water was larger. When 20% water was loaded, the reaction was not completed (68 mol% yield to **10**) even after 30 h. Nevertheless, no trace of carboxylic acid was found. Possibly if acid was formed it would rapidly react to give the methyl ester due to the presence of a Lewis acid. It seems that the presence of water may avoid metal–alcoholate adducts from forming on the active site (adsorption step) without which the reaction cannot occur and disfavours the hemiacetal formation.

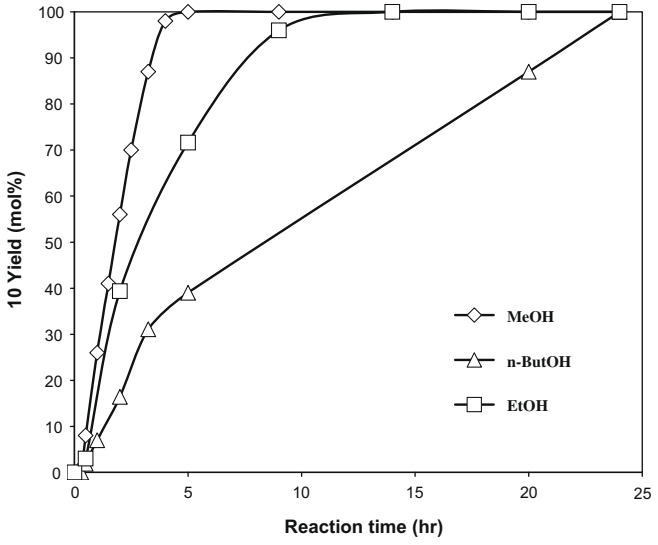

Fig. 8. Effect of the alcohol on the yield towards the corresponding ester from **1** at **1**/Au mol ratio 300, 130 °C and 10 bar bubbled O_2 using Au–CeO_2 catalyst. Acetals from acetaldehyde and butyraldehyde were also formed in high concentrations when EtOH and *n*-ButOH were used.

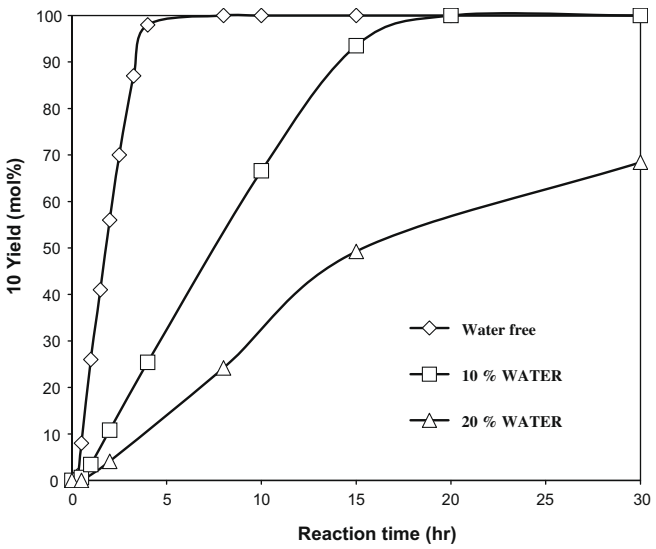

Fig. 9. Effect of water on **10** yield at **1**/Au mol ratio 300, 130 °C and 10 bar bubbled O_2 in MeOH using Au–CeO_2 catalyst.

4. Conclusions

Au–CeO_2 has proved to be an excellent catalyst for the aerobic oxidation of HMF into DMF and able to perform this reaction without base. Au–CeO_2 can be easily recovered and reused with small loss of activity but maintaining high selectivity towards DMF. Gold leaching was ruled out by means of chemical analysis of the material and the three-phase test. The reaction kinetics shows that the oxidative pathway encounters its limiting step for the oxidation of the alcohol to aldehyde. Once the aldehyde is formed, the corresponding hemiacetal is obtained, which is rapidly oxidized into the ester. From our results, we can conclude that the alcohol oxidation step is facilitated, if the 5-substituent group is a furane-ring activating function, in accordance with the previous results in the literature. Our study on the effect of temperature and the substrate to catalyst ratio demonstrates that the higher the temperature and the amount of catalyst gives rise to a higher initial reaction rate, but nevertheless 100% yield of DMF is always obtained. Unfortunately, any alcohol may not be suitable to carry out this oxidation, because they may also be oxidized and enter into a similar reaction pathway as the target reactant. Finally, water has a negative effect on the catalytic behaviour towards the formation of DMF, as it may impede adsorption of reactant onto the active site and subsequent oxidation.

Acknowledgments

The authors wish to acknowledge the Spanish Ministry of Education and Science for the financial support in the project MAT 2006-14274-C02-01 and the PROMETEO project of the Generalitat Valenciana. O.C. is grateful to the Spanish Council for Scientific Research (CSIC) for a Ph.D. scholarship.

References

[1] A. Corma, S. Iborra, A. Velty, Chem. Rev. 207 (2007) 2411.
[2] P. Mäki-Arvela, B. Holmbom, T. Salmi, D.Y. Murzin, Catal. Rev. 49 (2007) 197.
[3] G. Budroni, A. Corma, J. Catal. 257 (2008) 403.
[4] Y. Román-Leshkov, C.J. Barret, Z.Y. Liu, J.A. Dumesic, Nature 447 (2007) 982.
[5] K. Weissermel, H.J. Arpe, Industrial Organic Chemistry, VCH–Wiley, Weinheim, 1997, p. 255.
[6] C. Moreau, M.N. Belgacem, A. Gandini, Top. Catal. 27 (2004) 11.
[7] A. Fushiya, Japan Patent 075068 (2008).
[8] M.L. Ribeiro, U. Schuchardt, Catal. Commun. 4 (2003) 83.

[9] W. Partenheimer, V.V. Grushin, Adv. Synth. Catal. 343 (2001) 102.
[10] P. Verdeguer, N. Merat, A. Gaset, J. Mol. Catal. 85 (1993) 327.
[11] M. Kröger, U. Prüsse, K.D. Vorlop, Top. Catal. 13 (2000) 237.
[12] T. Mallat, A. Baiker, Chem. Rev. 104 (2004) 3037.
[13] K. Mori, T. Hara, T. Mizugaki, K. Evitan, K. Kaneda, J. Am. Chem. Soc. 126 (2004) 10657.
[14] W. Hou, N.A. Dehm, R.W.J. Scott, J. Catal. 253 (2008) 22.
[15] D.I. Enache, J.K. Edwards, P. Landon, B. Solsona-Espriu, A.F. Carley, A.A. Herzing, M. Watanabe, C.J. Kiely, D.W. Knight, G.J. Hutchings, Science 311 (2006) 4776.
[16] N. Dimitratos, A. Villa, D. Wang, F. Porta, D. Su, L. Prati, J. Catal. 244 (2006) 113.
[17] A. Abad, P. Concepción, A. Corma, H. García, Angew. Chem., Int. Ed. 44 (2005) 4066.
[18] A. Abad, C. Almela, A. Corma, H. García, Tetrahedron 62 (2006) 6666.
[19] A. Abad, A. Corma, H. García, Chem. Eur. J. 14 (2008) 212.
[20] A. Abad, C. Almela, A. Corma, H. García, Chem. Commun. (2006) 3178.
[21] A. Abad, A. Corma, H. García, Pure Appl. Chem. 79 (2007) 1847.
[22] A. Corma, H. García, Chem. Soc. Rev. 37 (2008) 2096.
[23] E. Taaring, I.S. Nielsen, K. Egeblad, R. Madsen, C.H. Christensen, Chem. Sus. Chem. 1 (2008) 75.
[24] F. Moreau, G.C. Bond, Appl. Catal. A: Gen. 302 (2006) 110.
[25] L. Zhang, S.A. Kozmin, J. Am. Chem. Soc. 126 (2004) 11806.
[26] F. Porta, L. Prati, M. Rossi, S. Coluccia, G. Martra, Catal. Today 61 (2000) 65.
[27] L.L. Santos, V.R. Ruiz, M.J. Sabater, A. Corma, Tetrahedron 64 (2008) 7902.
[28] P. Fristrup, L.B. Johansen, C.H. Christensen, Catal. Lett. 120 (2008) 184.
[29] Q. Fu, H. Saltsburg, M. Flytzani-Stephanopoulos, Science 301 (2003) 935.
[30] J. Guzman, S. Carretin, A. Corma, J. Am. Chem. Soc. 127 (2005) 3286.
[31] J. Guzman, S. Carretin, J.C. Fierro-González, L. Hao, B.C. Gates, A. Corma, Angew. Chem., Int. Ed. 44 (2005) 4778.
[32] B.H. Lipshutz, S. Tasler, W. Chrisman, B. Spliethoff, B. Tesche, J. Org. Chem. 68 (2003) 1177.
[33] I.W. Davies, L. Matty, D.L. Hughes, P.J. Reider, J. Am. Chem. Soc. 123 (2001) 10139.